ELSEVIER

Materials Chemistry and Physics 69 (2001) 274–277

MATERIALS CHEMISTRY AND PHYSICS

www.elsevier.com/locate/matchemphys

Materials Science Communication

Asymmetrical X-ray reflection of SiGeC/Si heterostructures

C.W. Liu [a,*], Y.D. Tseng [a], M.Y. Chern [b]

[a] *Department of Electrical Engineering, National Taiwan University, 1 Roosevelt Road, Sec. 4, Taipei 10764, Taiwan, ROC*
[b] *Department of Physics, National Taiwan University, 1 Roosevelt Road, Sec. 4, Taipei 10764, Taiwan, ROC*

Received 18 January 2000; received in revised form 15 March 2000; accepted 21 March 2000

Abstract

X-ray diffraction is widely used to measure the lattice parameters in the semiconductor heterostructures. For asymmetric reflection, both the glancing incident geometry and the glancing exit geometry satisfy the Bragg diffraction conditions. However, the rocking curves of these two diffraction geometries have different peak widths as well as different peak separations between the epilayer and the substrate. The direction of thickness broadening in the reciprocal lattice being not parallel to the normal of the reflection plane is responsible for the asymmetrical broadening in the rocking curve. An exact mathematical procedure is given to determine the lattice parameters of the epilayer from the normal reflex and one geometry of asymmetrical reflex. This procedure is very useful for some annealed SiGeC samples, since only glancing incident geometry can be measured.

The impressive progress in the growth [1,2] and characterization [3–5] of $Si_{1-x-y}Ge_xC_y$ alloys offers great flexibility to tailor the strain and the electronic properties of Group IV heterostructures [6–8]. Because the lattice constant of diamond (3.56683 Å [9]) is 34% smaller than that of Si, the substitutional incorporation of C can compensate the compressive strain of $Si_{1-x-y}Ge_x$ layers grown on Si substrates, where the lattice constant of Ge is 4.17% larger than that of Si. This increases the critical thickness of pseudomorphic $Si_{1-x-y}Ge_xC_y$ layers on Si. However, the formation of SiC precipitates at high temperature increases the compressive strain and leads to the misfit dislocation formation in the as-grown pseudomorphic $Si_{1-x-y}Ge_xC_y$ layers on Si with the thickness bellow its critical thickness [10]. To investigate the thermal stability of $Si_{1-x-y}Ge_xC_y$ alloys is important for further device applications. The in-plane lattice constant is a useful parameter to determine the relaxation of $Si_{1-x-y}Ge_xC_y$ layers on (1 0 0) Si.

The vertical lattice constant can be obtained from symmetrical (4 0 0) X-ray diffraction for the $Si_{1-x-y}Ge_xC_y$ layer grown on (1 0 0) Si. Fatemi and Stahlbush determined the in-plane and vertical lattice constants using two sets of asymmetrical reflections as well as the normal reflection [11]. The glancing incident geometry reveals a wider peak, compared to the glancing exit geometry, but no explanation has been given. Herzog and Kasper showed that any two independent reflections could be used to determine these two lattice constants with linearization approximation [12]. In this letter, we explain how the thickness broadening in the reciprocal lattice affects the diffraction peak width, and use a single set of asymmetric reflection as well as the normal reflection to obtain the in-plane and normal lattice constant using exact mathematical procedures.

The $Si_{1-x-y}Ge_xC_y$ epilayers used in this study were grown by rapid thermal chemical vapor deposition [2]. A typical (4 2 2) asymmetrical refection of 29 nm as-grown $Si_{0.701}Ge_{0.277}C_{0.022}$ on (1 0 0) Si is shown in Fig. 1. The peak width of the rocking curves for the glancing incident geometry is quite large, compared to the glancing exit geometry. In the reciprocal lattice, the diffraction condition [13] is $K_{in}-K_{out}=G$, where K_{in} is the incident wave vector, K_{out} the diffracted wave vector and G(4 2 2) the reciprocal lattice vector. The Ewald spheres can be used to visualize the diffraction condition with the same magnitude of K_{in} and K_{out} (Fig. 2a). There are two sets of solutions, corresponding to glancing incident geometry and glancing exit geometry, respectively. For the thin epilayer grown along with (1 0 0) direction, the reciprocal lattice point becomes broadened along the growth direction, not parallel with G(4 2 2) vector. If the broadening of G were along the direction of G vector, the broadening of the incident angle in the rocking curves would be the same (Fig. 2b). In fact, the broadening along the

* Corresponding author. Tel.: +886-2-23635251/515; fax: +886-2-23638247.
E-mail address: chee@cc.ee.ntu.edu.tw (C.W. Liu).

0254-0584/01/$ – see front matter
PII: S0254-0584(00)00271-6

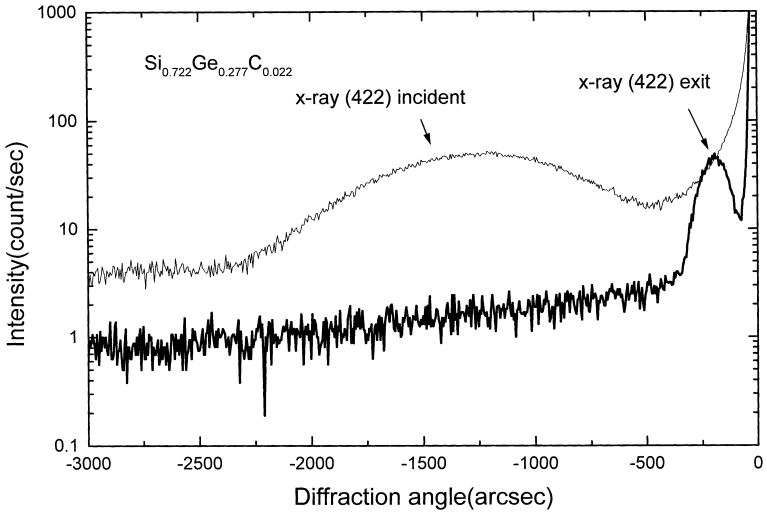

Fig. 1. A typical rocking curve for asymmetrical (4 2 2) diffraction. The sample is a 29 nm $Si_{0.701}Ge_{0.277}C_{0.022}$ layer grown on (1 0 0) Si. The peak for the glancing incident geometry is relatively strong and broad, while that for the glancing exit geometry is relatively narrow.

growth direction (1 0 0) yields smaller broadening of the incident angles for the glancing exit geometry, compared to the glancing incident geometry (Fig. 2c). The large peak width in the glancing incident geometry yields the uncertainty to determine the peak position of (4 2 2) reflection, while the narrow width in the glancing exit geometry makes this uncertainty of the peak position to be small. However, the relative weak intensity of the diffraction peak in the glancing exit geometry is very susceptible to the substrate interference.

The Bragg angle difference $\Delta\theta_B$ between the epilayer and the substrate for asymmetrical refection is one-half the sum of the measured incident angle separation of both geometries. Together with the symmetrical diffraction, the in-plane lattice constant can be obtained, as proposed by Fatemi and Stahlbush [11]. Two difficulties often occurred. The large broadening in the rocking curves for the glancing incident geometry causes some uncertainty to determine the exact location of the diffraction peaks (Fig. 1). Secondly, the weak diffraction peak for glancing exit geometry is very close to the substrate peak and sometimes cannot be measured due to the strong interference of the substrate peak, while the relatively narrow width of this peak can reduce the uncertainty to determine the peak position. We, therefore, proposed a new method to determine the in-plane lattice constant, based on only one of the asymmetrical diffraction geometry.

The misorientation $\Delta\phi$ and the angle between the (4 2 2) planes of epilayers and substrates is depending on the ratio between vertical lattice constant and in-plane lattice constant, i.e.

$$\Delta\phi = \arccos\left[\frac{4 + 2a_\perp/a_{||}}{(12(a_\perp/a_{||})^2 + 24)^{1/2}}\right] \quad (1)$$

In the rocking curve, the separation of the diffraction peaks between substrate and epilayer, Δ, can be expressed as

$$\Delta = \Delta\theta_B \pm \Delta\phi \quad (2)$$

where '+' is for the glancing incident geometry and '−' is for the glancing exit geometry. The vertical lattice constant is given by $a_\perp = 4d_{400}$, and in-plane lattice constant is

$$a_{||} = \left[\frac{8}{(1/d_{422}^2) - (1/d_{400}^2)}\right]^{1/2} \quad (3)$$

where d_{400} and d_{422} are the (4 0 0) and (4 2 2) plane distances of the epilayers, respectively. Besides (4 0 0) diffraction, only one set of diffraction (either glancing incident or glancing exit geometry) is sufficient to solve $a_\perp$ and $a_{||}$. The vertical lattice constant can be obtained from (4 0 0) diffraction. For a range of the initial value of in-plane lattice constant $a_{||,i}$, we can obtain the $\Delta\phi$ and $\Delta\theta_B$ from Eqs. (1) and (2), respectively. Finally, a range of final value of in-plane lattice $a_{||,f}$ can be obtained from Eq. (3). The intersection between the $a_{||,f}$ versus $a_{||,i}$ curve and the $a_{||,f} = a_{||,i}$ line is the in-plane lattice constant. Fig. 3 is a typical plot for such intersections for the $\Delta_e = 274$ arcsec in Fig. 2. There are two intersections and the larger one is not physically possible. Note that no linearization approximation is used to calculate the in-plane lattice constant.

A set of four $Si_{1-x-y}Ge_xC_y$ single quantum wells were used to test this new method. The samples were grown by rapid thermal chemical vapor deposition (RTCVD) using methylsilane as the carbon source. The first three $Si_{1-x-y}Ge_xC_y$ samples were grown at 625°C, and the last $Si_{1-x-y}Ge_xC_y$ sample is grown at 550°C. The samples were free of dislocations as measured by defect etching [10]. The pseudomorphic growth for these as-grown samples has been confirmed by the transmission electron microscope for samples grown on similar conditions [2]. These pseudomorphic layers have the same in-plane lattice constant as silicon substrate (5.43095 Å). The measured in-plane lattice constants are listed in Table 1, obtained from Fatemi and Stahlbush's method, the glancing incident geometry, and

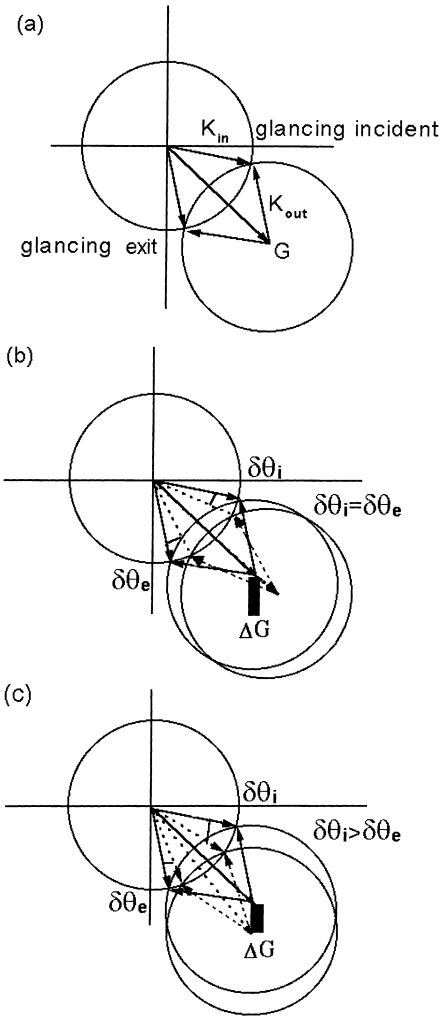

Fig. 2. Ewald sphere construction to illustrate the different peak width between the glancing incident and the glancing exit geometry. (a) The two solutions are corresponding to these two diffraction geometry; (b) the broadening would be the same, if the growth direction was along the reciprocal vector; (c) the thickness broadening along the growth direction, not parallel with reciprocal vector, yields different peak width of the diffraction peaks.

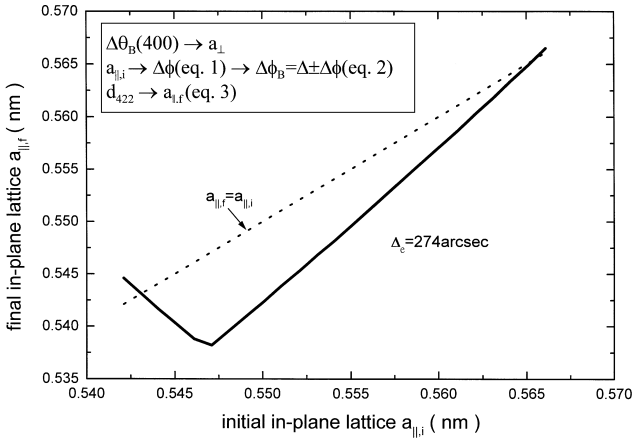

Fig. 3. The plot to get the solution of the in-plane lattice constant. The one solution of larger lattice constant is not physically possible. The inset is the procedure to obtain the $a_{||,f}$ vs. $a_{||,i}$ curve.

the glancing exit geometry. The measurement uncertainty of the in-plane lattice constant is also listed in Table 1, as compared to the Si lattice constant. The accuracy of the new proposed methods is at least as good as the Fatemi and Stahlbush's method. The average uncertainties are 1.0×10^{-4}, 1.2×10^{-4}, and 1.4×10^{-4} for the glancing exit geometry, the glancing incident geometry, and Fatemi and Stahlbush's method, respectively. This result is expected, since the narrow peak width of the glancing exit geometry reduces the uncertainty to determine the peak locations.

When the thin samples (the first three samples) were annealed at high temperature 1000°C for 2 h, the (4 2 2) diffraction peak in the glancing exit geometry cannot be measured due to the weak intensity of this peak as well as strong substrate interference. The usefulness of this method can be demonstrated, since the peak position in the glancing incident geometry is sufficient to determine the in-plane lattice constant. The results are given in Table 2. The in-plane lattice constant increases after annealing, indicating that the $Si_{1-x-y}Ge_xC_y$ layer were relaxed. The in-plane lattice constant increases as the amount of carbon incorporation increases after the 1000°C annealing for 2 h. The silicon carbide precipitates may be responsible for the relaxation [10].

We have proposed a method to determine the in-plane lattice constant of stained layers. Only one of the asymmetrical diffraction conditions is required in this method. The Ewald spheres are proposed to explain the different peak widths for these two diffraction conditions. This method is applied to pseudomorphic $Si_{1-x-y}Ge_xC_y$ layers grown on Si. The accuracy of the resulting in-plane lattice constant has at least the same accuracy as the previous method. For

Table 1
The measurement results of Fatemi and Stahlbush's method, the glancing incident geometry, and the glancing exit geometry[a]

$Si_{1-x-y}Ge_xC_y$ (thickness in nm)	Δ_i (arcsec)	Δ_e (arcsec)	$\Delta\theta_B$ (arcsec)	$a_{\|\|}$ from $\Delta_e+\Delta_i$[b] (Å)	$a_{\|\|}$ from Δ_i[b] (Å)	$a_{\|\|}$ from Δ_e[b] (Å)
$Si_{0.758}Ge_{0.23}C_{0.012}$ (18)	1580	274	970	5.43253 (2.91×10^{-4})	5.43131 (6.63×10^{-5})	5.43197 (1.88×10^{-4})
$Si_{0.762}Ge_{0.23}C_{0.008}$ (23)	2425	386	1501	5.43135 (7.37×10^{-5})	5.43163 (1.25×10^{-4})	5.43153 (1.07×10^{-4})
$Si_{0.77}Ge_{0.23}$ (24)	3477	506	2144	5.4303 (1.20×10^{-4})	5.43203 (1.99×10^{-4})	5.43063 (5.89×10^{-5})
$Si_{0.701}Ge_{0.277}C_{0.022}$ (29)	1272	192	787	5.43054 (7.55×10^{-5})	5.43143 (8.84×10^{-5})	5.43070 (4.60×10^{-5})

[a] The average measurement uncertainties are 1.0×10^{-4}, 1.2×10^{-4}, and 1.4×10^{-4} for the glancing exit geometry, glancing incident geometry, and Fatemi and Stahlbush's method, respectively.

[b] The numbers in parentheses indicate the uncertainty, as compared to Si lattice constant. All the films are pseudomorphic.

Table 2
The measurement results of the glancing incident geometry for the samples annealed for 2 h at 1000°C[a]

$Si_{1-x-y}Ge_xC_y$ (thickness in nm)	Δ_i (arcsec)	$\Delta\theta_B$ (arcsec)	$a_{\|\|}$ from Δ_i (Å)
$Si_{0.758}Ge_{0.23}C_{0.012}$ (18)	1515	1069	5.44272
$Si_{0.762}Ge_{0.23}C_{0.008}$ (23)	1996	1484	5.44155
$Si_{0.77}Ge_{0.23}$ (24)	2400	2166	5.43980

[a] Only the diffraction in the glancing incident geometry can be measured.

some $Si_{1-x-y}Ge_xC_y$ samples annealed at high temperature, the diffraction peak in the glancing exit geometry cannot be measured. Our method can be used in this situation.

Acknowldgements

This work was supported by National Science Council (NSC 88-2218-E-002-004). The authors would also like to thank the group of Prof. James Sturm at Princeton University for supplying the samples.

References

[1] J.L. Regolini, F. Gisbert, G. Dolino, P. Boucaud, Mater. Lett. 18 (1993) 57.
[2] C.W. Liu, A. St. Amour, J.C. Sturm, Y.R.J. Lacroix, M.L.W. Thewalt, C.W. Magee, D. Eaglesham, J. Appl. Phys. 80 (1996) 3043.
[3] P. Boucaud, C. Francis, F.H. Julien, J.-M. Lourtioz, D. Bouchier, S. Bodnar, B. Lambert, J.L. Regolini, Appl. Phys. Lett. 64 (1994) 875.
[4] A. St. Amour, C.W. Liu, J.C. Sturm, Y. Lacroix, M.L.W. Thewalt, Appl. Phys. Lett. 67 (1995) 3915.
[5] C.Y. Lin, C.W. Liu, Appl. Phys. Lett. 70 (1997) 1441.
[6] L.D. Lanzerotti, A. St. Amour, C.W. Liu, J.C. Sturm, J.K. Watanabe, N.D. Theodore, IEEE Electron Device Lett. 17 (1996) 334.
[7] I.M. Anteney, G. Lippert, P. Ashburn, H.J. Osten, B. Heinemann, G.J. Parker, D. Knoll, IEEE Electron Device Lett. 20 (1999) 116.
[8] S. John, S.K. Ray, E. Quinones, S.K. Oswai, S.K. Banerjee, Appl. Phys. Lett. 74 (1999) 847.
[9] O. Maselung, Semiconductor — Basic Data, 2nd Edition, Springer, Berlin, 1996, p. 7.
[10] C.W. Liu, Y.D. Tseng, M.Y. Chern, C.L. Chang, J.C. Sturm, J. Appl. Phys. 85 (1999) 2124.
[11] M. Fatemi, R.E. Stahlbush, Appl. Phys. Lett. 58 (1991) 825.
[12] H.-J. Herzog, E. Kasper, J. Crystal Growth 144 (1994) 177.
[13] N.W. Ashcroft, N.D. Mermin, Solid State Physics, Saunders College, Philadelphia, 1976, p. 99.